Carious growth monitoring with optical coherence tomography

A. Z. Freitas[*a], D. M. Zezell[a], M.P.A. Mayer[b], A. C. Ribeiro[c], A. S. L. Gomes[d], and N. D. Vieira Jr[a]
[a]Centro de Lasers e Aplicações, Instituto de Pesquisas Energéticas e Nucleares, Av. Lineu Prestes, 2242, - CEP. 05422-950 - Cidade Universitária "Armando de Salles Oliveira" - São Paulo – Brazil
[b]Instituto de Ciências Biomédicas: Av. Prof. Lineu Prestes, 2415 - São Paulo -SP -CEP:05508-900
[c]Faculdade de Odontologia da Universidade de São Paulo – Av.Lineu Prestes, 2227 - Cidade Universitária –São Paulo – SP - Brazil
[d]Departamento de Física, Universidade Federal de Pernambuco, Av. Professor Luiz Freire, s/n Cidade Universitária, 50670-901, Recife - Pernambuco – Brazil

ABSTRACT

Optical Coherence Tomography was used to monitor subsurface caries evolution process *in vitro*. Human tooth was used and bacteria were employed to induce caries lesions. Twenty-five human third molars, were used in this study. The teeth were cut longitudinally at mesio-distal direction; the surfaces were coated with nail varnish except for two squared windows (2x4 mm); at the cement-enamel junction. Artificial lesions were induced by a *S. Mutans* microbiological culture. The samples (N = 50) were divided into groups according to the demineralization time: 3, 5, 7, 9 and 11 days. The culture medium, was changed each 48 hours. After the demineralization process the samples were rinsed with double-deionized water and stored in a humid environment. The OCT system[1] was implemented with average power of 96 μW in the sample arm, providing a 23 μm of axial resolution. The images were produced with lateral scans step of 10 μm. The detection system was composed by a detector, a demodulator and a computer. With the images generated by OCT it was possible to determine the lesion depth as function of sample exposition time to microbiological culture. We observed that the depth of the lesion in the root dentine increased from 70 μm to 230 μm, depending of exposure time, and follows the bacterial population growth law. This OCT system accurately depicts hard dental tissue and it was able to detect early caries in its structure, providing a powerful contactless high resolution image of lesions.

Keywords: Optical coherence tomography, caries, diagnostic imaging, backscattering

1. INTRODUCTION

The application of optical technologies in medicine and biology has a long history. Since the 18th century, the microscope has been an indispensable tool for biologists. With the invention of the laser in 1960, physicians greatly benefited from less invasive surgical procedures. The development of fiber optics led to the manufacture of endoscopes, allowing direct view of internal organs deep in the body with minimal invasion. Optical technologies enable easy chemical analysis of tissue samples and the counting and measuring blood cells. In spite of these and other advances, few of the optical instruments used today in medicine take full advantage of the coherence properties of light.

Optical coherence tomography (OCT) is a diagnostic imaging technology in which the coherence features of photons are exploited, leading to a imaging technology that is capable of producing high resolution cross-sectional images of the internal microstructure of living tissue. Its applications in medicine were reported less than a decade ago[2,3,4], but its roots lie in early works on white-light interferometry, that led to the development of optical coherence-domain reflectometry (OCDR), a one dimensional (1-D) optical ranging technique[5].

Although OCDR was originally developed for finding faults in optic fiber cables and network components, its capability to probe the human eye structure[6,7] and other biological tissues[8,9] was readily identified. The optical sectioning ability of OCT, due to the short temporal coherence of a broadband light source, enables OCT scanners to image microscopic tissue structures at depths beyond the conventional bright-field and confocal microscopes.

Lasers in Dentistry XII, edited by Peter Rechmann, Daniel Fried, Proc. of SPIE Vol. 6137, 613704, (2006) · 1605-7422/06/$15 · doi: 10.1117/12.646131

Currently, dentists evaluate the oral health of a patient through three main methods: visual/tactile examination, periodontal probing, and radiographic imaging. Probes are placed between the soft tissue and tooth to assess periodontal conditions. The probe penetration depth is measured and the location of the soft tissue attachment is estimated from a fixed reference point on the tooth. This method can be painful and its diagnostic is imprecise due to variations on insertion force, inflammatory status of tissue, diameter of probe tips, and anatomical tooth contours[10]. Radiographies reveal structural characteristics of teeth and bone that can not be identified in a visual examination. While radiographies are highly sensitive to detecting regions of significant carious demineralization and bone loss, they have several limitations in identifying periodontal diseases as they provide no information about soft tissue. Also, they are two dimensional and the precise position of a carious lesion is very difficult or even impossible. In addition, radiography uses potentially harmful ionizing radiation and can not provide information about soft tissue state.
The goal of this work is to use the OCT technique to produce in vitro tomographic images of dental microstructure that can be used to make both qualitative and quantitative analysis of dental health. In particular, we found that carious region depth grows with logarithmic profile, suggesting that it follows the bacteria growth law.

2. METHODOLOGY

2.1. System configuration

The configuration employed in the OCT system was the "open air" Michelson interferometer illustrated in Figure 1.

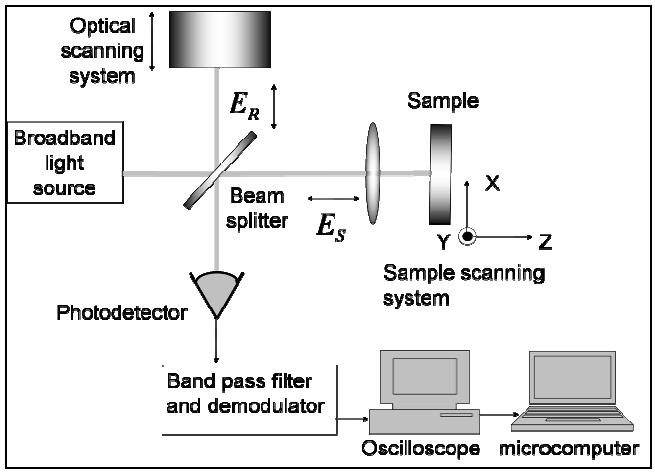

Figure 1 Critical components of a standard OCT system

In this type of interferometer, light from the source propagates through a 50/50 beam-splitter, where half of the optical intensity is transmitted to the delay line. The remaining half of the light is directed to the sample. The light source was a mode locked Ti:Sapphire laser (Mira - Coherent) centered around 830 nm with 51 fs pulse width and 20 nm FWHM spectral width. The autocorrelation trace shown Figure 2, was measured with an autocorrelator (home made), and in Figure 3 the spectral distribution measured with a fast spectrometer (Positive Light - ULS).

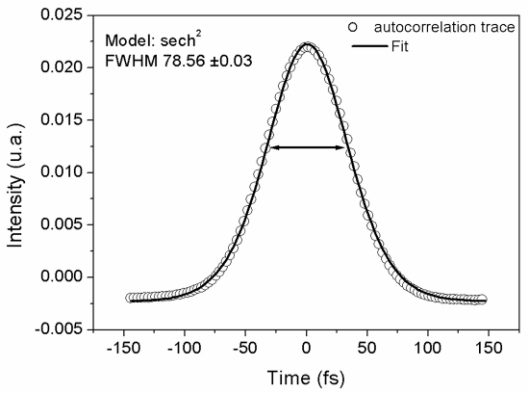

Figure 2 Autocorrelation trace for laser pulse. The pulse width was 51 fs.

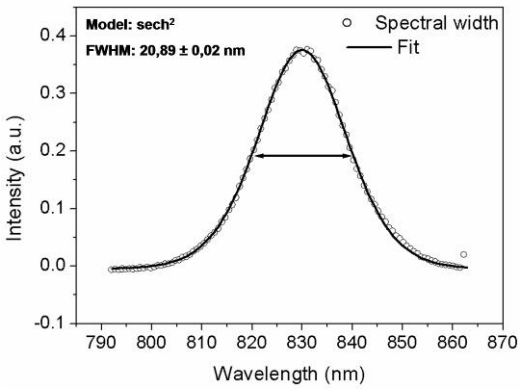

Figure 3 Spectrum of Ti:Sapphire laser (Mira) centered around 830 nm

The lasers system provided an average power 100 mW (Ophir PowerMeter) at a repetition rate of 76 MHz. The delay line, Fast Fourier Scanning, was implemented with a scanner (General Scanning 6120D) operating at a frequency of 200 Hz, a grating with 590 lines/mm (p = 1.69 μm), 25x25 mm lateral dimensions, and a lens with 50 mm of focal length. The maximum angular excursion of the scanning mirror was set to produce a usable group delay scan of approximately Δl_g = 1.0 mm. A low noise amplified detector (SR-194) with an electronic circuit detecting only the positive part of signal, as shown in Figure 4, was used. A digital oscilloscope was employed to display the data (Tektronix 3000B) and subsequently stored onto a personal computer. To displace the sample in the X axis, in order to obtain an image, we use a computer controlled translation stage (Thorlabs, T25-XYZ) with minimum step of 0.05 μm.

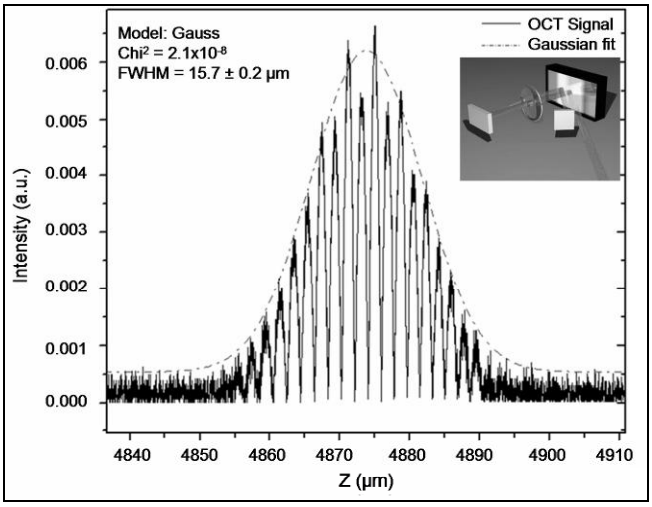

Figure 4 OCT signal, used for calibration, obtained with a mirror as the sample. Inset shows a view of the optical delay line. The beam is diffracted by the grating and collimated by the lens in the scanning mirror

2.2. Sample Preparation

Fifteen human third molars extracted for orthodontic reasons were used in this study. After the surgical procedure, the teeth were cleaned under tap water to remove the organic debris. Then, they were immersed in deionized water and kept under refrigeration until use.

The teeth were cut longitudinally through the mesio-distal direction. The buccal and lingual surfaces were cleaned up, dried and covered with resistant nail varnish except at squared windows (2 x 4 mm) shown in Figure 5.

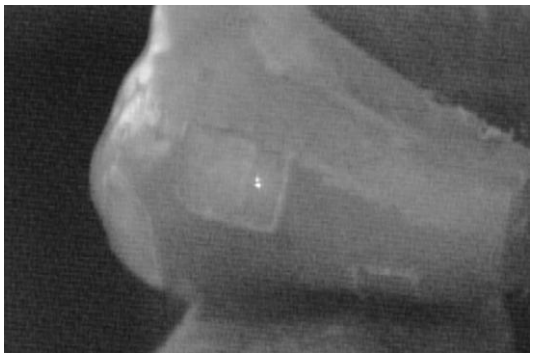

Figure 5. Square window exposed after cover the tooth with nail varnish

A total of 111 samples were submitted to the demineralization process for different experimental times, distributed at the enamel surface (n = 36), the enamel-cementum junction (n = 58) and at root surface (n = 17). Each sample was individually fixed at the depth of a well of 24 wells acrylic tissue culture plate and sterilized by gamma rays (25 KGy).

2.3. Microbiological procedure

Demineralization of the teeth surfaces was performed using *S. mutans* strain GS5 in a sucrose rich medium. Briefly, a 1 ml aliquot of a standard culture of the bacteria in tryptic soy broth (Difco) added with 5% sucrose and 0.01% Potassium tellurite medium grown for 18 hs in 10% CO_2 at 37°C was added to each well. The plates were incubated in a CO_2 incubator containing 10% CO_2, at 37°C for different periods of times (3, 5, 7, 9 and 11 days). The used medium containing planctonic bacterial cells was removed every 48 hs, and a fresh sterile medium was added to the well containing the teeth fragments covered by the S. mutans biofilm.

2.4. Microscopic analysis

After the teeth samples had been analyzed by the OCT technique, they were prepared to the microscopic analysis aiming to determine the lesion depth. The demineralized regions were sectioned with a diamond disk at approximately the same point analyzed by the OCT. This position was determined by visual inspection with help of a snapshot video image (Figure 6) showing the laser incident points, and by positioning the disk perpendicularly to the teeth surface in order to acquire slices of about 400 μm. The fragments were washed and immersed in quinoline (SIGMA) overnight. The slices were examined under the microscope by polarization light at 5X (Leika DMLP). The microscope images were captured by a digital camera and the lesion depth measured with software program (Image J).

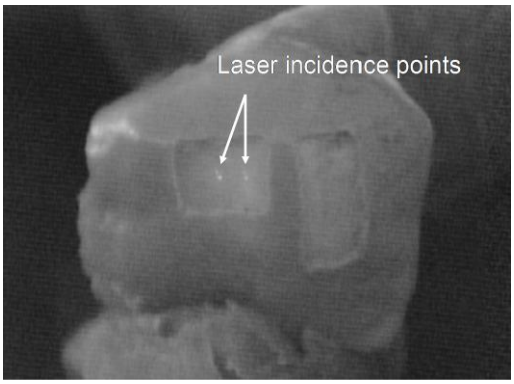

Figure 6 Frame of video image captured to define the position of OCT scan region, for optical microscopy analysis

2.5. Image formation

The OCT cross section images, e.g. Figure 7, was constructed using the depth-priority scanning protocol (A-scan), where axial scans are acquired at successive transverse positions. The tooth was moved laterally, perpendicular to the laser axis, in 10 μm increments. All scans were normalized to a maximum OCT signal (front surface) and a false-color gray scale was used. To obtain the results shown in Figure 10, transverse images sections from different positions of the sample in the Y axis (Figure 1) were grouped. The construction was accomplished with the aid of analysis software and voxel visualization (VGStudio Max 1.2). This three-dimensional re-construction allows transversal sections analysis different from those obtained directly from the OCT system.

3. RESULTS

The optical coherence tomographic images were produced, showing that it is possible to depict internal structure of dental tissue. In particular it was shown that it is possible to detect early artificial caries. Figure 7 shows the structure of a carious region of one tooth with 11 days of demineralization time, on the left side of the figure we have the enamel showing the carious region and on the right side, cementum region, shows smaller backscattering signal between the tooth surface and body of lesion, the distance was measured and corrected by refraction index of tooth[11] (1.62 @ 856 nm), which is in agreement with the optical microscope image Figure 8.

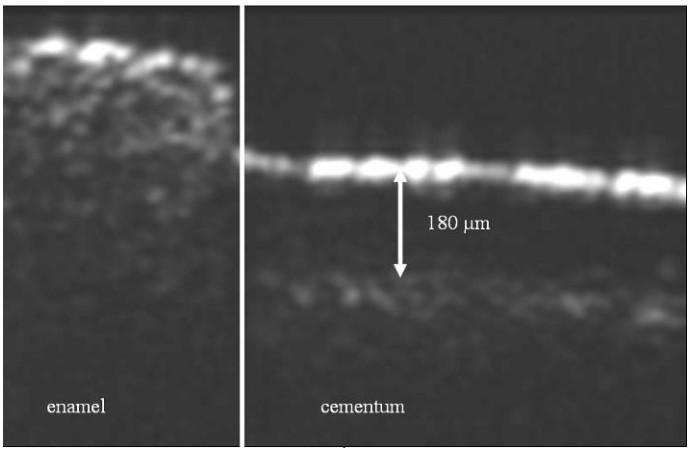

Figure 7 OCT image of tooth submitted to the demineralization process for 11 days

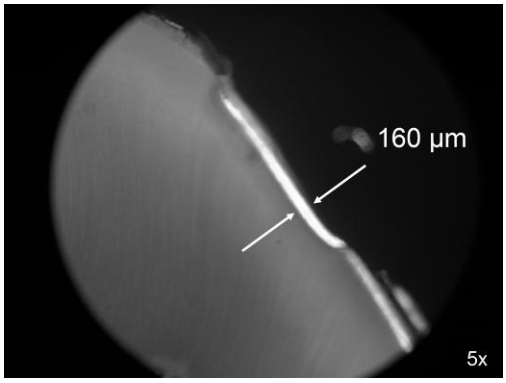

Figure 8 Visible polarized micrograph of sample with 11 days of exposition time, showing the carious region

The cross section optical coherence tomographic images showing in, Figure 9, clearly shows the demineralization process taking place in the teeth as function of exposition time to bacteria culture, carious region have signal deeper than sound region and depends on the demineralization time. In this region the backscattering coefficient is smaller, allowing a larger penetration of the laser in the sample. This set of figures represents one image of each time of demineralization.

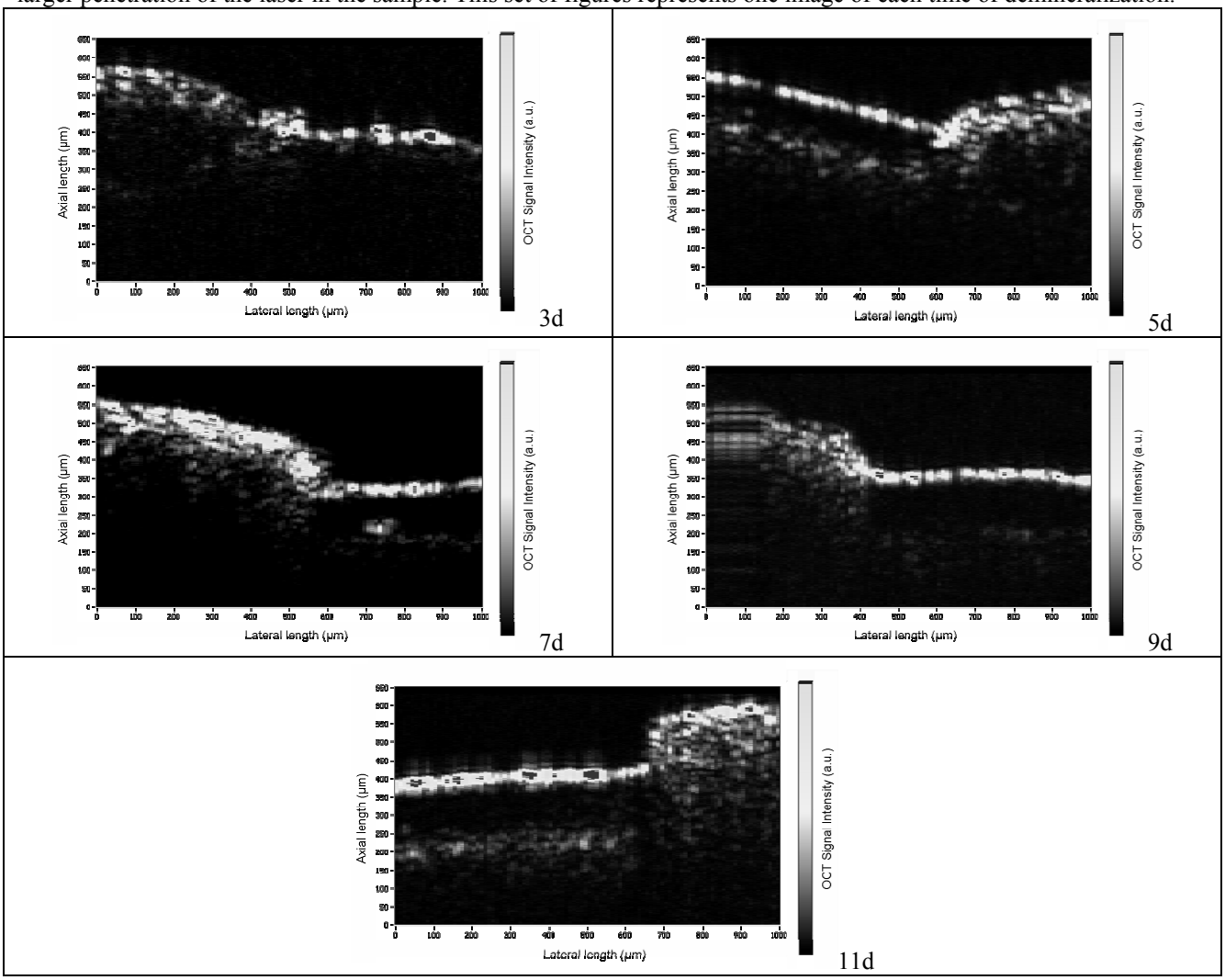

Figure 9 OCT images at enamel-cementum junction for teeth with 3, 5, 7, 9, and 11 days of demineralization process, showing the evolution of the carious region depth

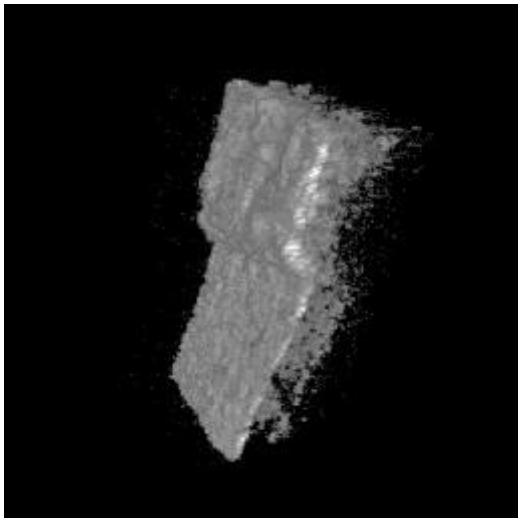

Figure 10. Three-dimensional image construction of lesion region in tooth with 11 days exposition time

Figure 11 shows distances measured in OCT images, from tooth surface to the back limit of body lesion, for different time of demineralization, following a typical bacteria growth law. When growing exponentially by binary fission, the increase in a bacterial population is given by geometric progression, $b = B \times 2^n$ where B = number of bacteria at the beginning of a time interval, b = number of bacteria at the end of the time interval, n = number of generations (number of times the cell population doubles during the time interval). Solving for n, the equation becomes:

$$n = \frac{\log b - \log B}{\log 2} = 3.3 \log\left(b / B\right) \tag{1}$$

Exponential growth cannot be continued for long period in a batch culture[12] (e.g. a closed system such as a test tube or flask). Population growth is limited by one of three factors: 1. exhaustion of available nutrients; 2. accumulation of inhibitory metabolites or end products; 3. exhaustion of space, in this case called a lack of "biological space". During the stationary phase, if viable cells are being counted, it cannot be determined whether some cells are dying and an equal number of cells are dividing, or the population of cells has simply stopped growing and dividing. Of course the growth of carious region depth, do not follow exactly this law because the process is much more complex, involving dynamic Ca (calcium) and P (phosphorus) uptake and release from solution, but it can seen that the data follows the same shape.

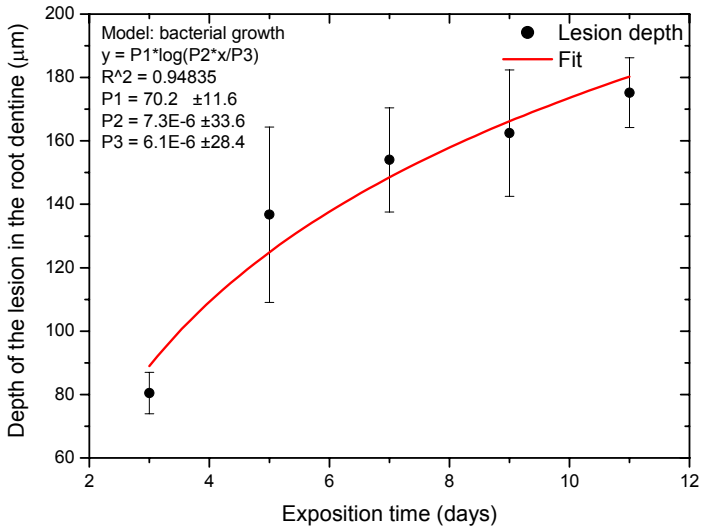

Figure 11 Progression of depth lesion in the root dentine as function of exposition time

4. CONCLUSIONS

The OCT system provides a powerful contactless and noninvasive diagnostic method and could be used to replace, or complement, the traditional diagnostic methods such as X-ray radiography, avoiding potentially hazardous ionization radiation and enabling 3D images to be generated, showing that it is possible to image internal structure of dental tissue.
It is important to emphasize that the optical changes in carious tissue can be readily detected by the OCT, before structural changes become apparent by conventional detection methods.
In this work an OCT system with a Fast-Fourier scan delay line was implemented with average power of 96 µW in the sample arm, providing a 23 µm of axial resolution. In particular it was shown due to its spatial resolution and contrast that it is possible to detect early artificial caries. The images generated by OCT made possible to determine the lesion depth as function of sample exposition time to microbiological culture (demineralization). We observed that the depth of the lesion in the root dentine increased from 70 µm to 230 µm, for 3 days to 11 days of demineralization time, and follows the bacterial population growth law. This OCT system accurately depicts hard dental tissue and it was able to detect early caries in its structure, providing a powerful contactless high resolution image of lesions. A complete set of experiment under way taken a count other variables during the demineralization process like pH measure and population counting, in other to explain the processes evolved more precisely.

ACKNOWLEDGMENTS

This research was supported by FAPESP (grant # 00/15135-9).

REFERENCES

[1] Freitas, A.Z.; Zezell, D.M.; A. C. Ribeiro, A.C.; Gomes, A. S. L. and Vieira Jr., N. D. "Imaging carious human dental tissue with optical coherence tomography", J. Appl. Phys., **99**, (2006) (to be published)
[2] J. G. Fujimoto, M. E. Brezinski, G. J. Tearney, S. A. Boppart, B. E. Bouma, M. R. Hee, J. F. Southern, and E. A. Swanson, "Optical biopsy and imaging using optical coherence tomography", Nature Med., **1**, 970-972 (1995).
[3] A. F. Fercher, C. K. Hitzenberger, W. Drexler, G. Kamp, and H. Sattmann, "In vivo optical coherence tomography", Amer. J. Ophthalmol., **116**, 113-114 (1993).
[4] R. C. Youngquist, S. Carr, and D. E. N. Davies, "Optical coherence domain reflectometry: A new optical evaluation technique", Opt. Lett., **12**, 158-160 (1987).
[5] K. Takada, I. Yokohama, K. Chida, and J. Noda, "New measurement system for fault location in optical waveguide devices based on an interferometric technique", Appl. Opt., **26**, 1603-1606 (1987).
[6] A.F. Fercher, K. Mengedoht, and W. Werner, "Eye-length measurement by interferometry with partially coherent light", Opt. Lett., **13**, 1867-1869 (1988).
[7] J. A. Izatt, M. R. Hee, E. A. Swanson, C. P. Lin, D. Huang, J. S. Schuman, C. A. Puliafito and J. G. Fujimoto, "Micrometer-scale resolution imaging of the anterior eye with optical coherence tomography", Arch. Ophthalmol., **112**, 1584-1589 (1994).
[8] W. Clivaz, F. Marquis-Weible, R. P. Salathe, R. P. Novak, and H. H. Gilgen, "High-resolution reflectometry in biological tissue", Opt. Lett., **17**, 4-6 (1992).
[9] J. M. Schmitt, A. Knüttel, and R. F. Bonner, "Measurement of optical properties of biological tissues by low-coherence reflectometry", Appl. Opt., **32**, 6032-6042 (1993).
[10] L. Mayfield, G. Bratthall and R. Attstrom, "Periodontal probe precision using four different periodontal probes", J. Clin. Periodontology, **23**, 76-82 (1996).
[11] Xiao-Jun Wang, Thomas E. Milner, Johannes F. de Boer, Yi Zhang, David H. Pashley, and J. Stuart Nelson "Characterization of dentin and enamel by use of optical coherence tomography" Applied Optics, **38** (10), 2092 (1999)
[12] D. K. Button, "Kinetics of Nutrient-Limited Transport and Microbial Growth", Microbiol. Rev., **49** (3), 270-297 (1985)

* azanardi@ipen.br, skype name: azanardi, www.ipen.br